sustainability

MDPI

Article

CO_2 Emissions from Blade Waste Treatments under Wind Power Scenario in Japan from 2021 to 2100

Shota Nogaki, Lisa Ito *, Toyohiko Nakakubo and Akihiro Tokai

Graduate School of Engineering, Osaka University, 2-1 Yamadaoka, Suita 565-0871, Japan; nogaki@em.see.eng.osaka-u.ac.jp (S.N.); nakakubo@see.eng.osaka-u.ac.jp (T.N.); tokai@see.eng.osaka-u.ac.jp (A.T.)

* Correspondence: lisa.ito@see.eng.osaka-u.ac.jp; Tel.: +81-6-6879-7678

Abstract: Wind power generation has been introduced to reduce carbon emissions; however, recycling or recovering the waste of wind blades, which contain fibre-reinforced plastic, is difficult. Converting the recovered materials for secondary use is also difficult owing to the decreased strength and low material value. Many countries, including Japan, have not considered the future energy and CO_2 emission scenarios, particularly CO_2 emissions from wind blade waste. Based on these scenarios, Japan has planned to introduce large amounts of onshore/offshore wind power generation through 2050. Therefore, we aimed to evaluate quantitatively the total amount of waste and the global warming potential (GWP) from multiple blade waste treatment processes. Based on the average lifetime of blades (20–25 years), we found that the GWP of wind blade waste treatment in Japan may reach a maximum of 197.3–232.4 $MtCO_2eq$ by 2060–2065. Based on this lifetime, the wind blade treatment in 2050 accounted for 63.9–80.1% of the total greenhouse gas emissions in 2050. We also showed that the rise in CO_2 emissions from the wind blade wastes would make up 82.5–93.6% of the potential reduction in the GWP, which is achievable by shifting from thermal to wind power generation.

Keywords: wind power generation; waste treatment; fibre-reinforced plastic; recycling; CO_2 emissions; scenario analysis

Citation: Nogaki, S.; Ito, L.; Nakakubo, T.; Tokai, A. CO_2 Emissions from Blade Waste Treatments under Wind Power Scenario in Japan from 2021 to 2100. *Sustainability* **2024**, *16*, 2165. https://doi.org/10.3390/su16052165

Academic Editor: Alessio Siciliano

Received: 29 January 2024
Revised: 22 February 2024
Accepted: 1 March 2024
Published: 5 March 2024

1. Introduction

At present, the introduction of renewable energy is being promoted in electric power sectors worldwide to respond to the issue of climate change [1]. In 2022, global wind power generation increased by 265 TWh, reaching 2100 TWh [International Energy Agency (IEA) [1]]. By 2030, more than 500 GW of new renewable energy is planned to be added [1,2]. Among renewable energy sources, solar power generation is becoming more prominent, while wind power generation is also being developed not only onshore but also offshore [3]. Furthermore, many countries have ratified the Paris Agreement adopted at COP21 [4]. The Intergovernmental Panel on Climate Change (IPCC) has been conducting multiple scenario analyses and presented the low energy demand (LED) scenario in its integrated report in 2019 [5].

However, wind power generation equipment has a lifetime, and a large amount of waste is predicted to be produced at the end of that lifetime [6–9]. The previous study established multiple-scenario life cycle stages, such as manufacturing and operation and management (O&M), of wind power generation [6].

With regard to wind power generation, the disposal of waste from wind blades is considered a problem [6]. Wind blades are made from glass-fibre-reinforced plastic (GFRP) and carbon-fibre-reinforced plastic (CFRP), which are extremely lightweight, allowing for the production of strong structural components [10]. To date, several previous studies have discussed how wind blades can be disposed of at the end of their lifetime, including landfilling after cutting, incineration, thermal recycling (energy recovery), mechanical recycling, and chemical recycling [10–18]. However, given the physical properties of

GFRP/CFRP, two challenges exist in the recycling of materials and making secondary use of recovered materials. The first problem is a decrease in the strength of recycled materials. GFRP and CFRP cannot be reformed because they are cross-linked [19], and obtaining the same strength as the primary material is difficult for materials recovered through mechanical recycling [16]. The strength of recycled glass materials recovered through thermal recycling can be reduced by up to 80% [20]. The second issue is the low economic incentive for recycling. The cost competitiveness of materials obtained by recycling is low [21]. The widespread use of materials recovered from mechanical recycling requires significant financial support [7]. Chemical recycling can be costly compared with other methods [20]. For these reasons, incineration and landfilling have been suggested to continue as the primary treatment options for wind blade waste [9,17,18]. Even if wind blade waste is recycled, a possibility exists that the recovered materials will not be properly recycled.

Japan is one of the world's largest energy consumers and importers, and it relies on imports from other countries for nearly 96% of its primary energy supply at the national level [22]. Thermal power generation accounts for 72% of Japan's electricity sector and is seen as a challenge [23]. In 2020, the country declared that it will aim for carbon neutrality (a concept that means net zero in terms of greenhouse gas [GHG] emissions and absorption) by 2050 [24]. To achieve carbon neutrality, effort in the energy sector, which emits 85% of GHGs, is important, and Japan's 6th Basic Energy Plan sets the goal of rapidly increasing renewable energy use in the power sector in the future [25]. To achieve this goal, Japan is conducting multiple energy scenario analyses to review its power source mix with the aim of achieving decarbonisation by 2050 [26–29]. At present, solar power generation in Japan is being introduced through subsidy systems, such as the feed-in tariff (FIT) system, which started in 2012, and the amount of solar power generation rapidly increased from 6613 GWh to 94,801 GWh from 2012 to 2022 [1]. Meanwhile, the amount of wind power generation in 2022 was 9603 GWh [1], and the introduction of wind power generation has been delayed. In the future, plans are underway to introduce not only onshore wind power but also offshore wind power in large quantities, and wind power generation is predicted to increase [3].

Therefore, the waste generated from solar power generation and wind power generation equipment, which is discharged after its lifetime ends, should be considered. Regarding waste treatment for solar power generation, only a few countries other than the European Union market regulate waste solar panels; however, Japan is actively involved in the research and development of recovery technologies and manufacturers' recycling effort [30]. In Japan, where the large-scale introduction of wind power generation is predicted to occur in the future [31], no studies (to the authors' knowledge) have yet predicted the future amount of wind blade waste and CO_2 emissions from its treatment processes. Furthermore, wind blade waste from wind power generation has not been considered in multiple energy scenario analyses for Japan [29,31] that are currently being conducted. After considering Japan's unique wind power generation lifetime, estimating the future disposal timing of wind blades and the amount of CO_2 emitted during their disposal from the energy scenarios [5,31] devised by IPCC is important to achieve low carbon emissions in the future. In addition, by considering the blade waste generated from all stages of a wind blade's life cycle (manufacturing, service, and end-of-life stages), estimating the total amount of wind blade waste is possible. Japan, where the wind power generation industry is not yet fully developed, is currently engaged in debates on how to dispose of blade waste, referring to Europe and other countries with advanced wind power generation sectors [32].

Therefore, the objective of this study is to quantitatively estimate the total amount of waste emitted during each life cycle of wind blades (from manufacturing to disposal) and the amount of waste disposed of when large quantities of onshore/offshore wind power are introduced in Japan towards achieving a low-carbon society. When calculating the CO_2 emissions of the blade waste treatment process, European recycling or treatment processes [10–14] were considered.

Recycling methods for GFRP/CFRP, which constitute wind blade waste, have been studied [10,12–14,16]. However, the recovered materials have low material strength [16,19,20], and economic incentives are small [7,20,21], so recycling methods are not widely accepted by society [9,17,18]. Therefore, in this study, CO_2 benefits from secondary use were not included in the system boundary, and the global warming potential (GWP) [tCO_2eq] was calculated quantitatively to predict CO_2 emissions in line with the actual situation.

2. Materials and Methods

2.1. Research Flow and Life Stages of Blade Waste

In this study, we estimated the installed/decommissioned capacity of onshore/offshore wind power up to the year 2100 based on the 2050 decarbonisation scenario for Japan (Section 2.2). We investigated past trends in wind power generation facilities in Japan during that period from wind power generation facility data provided by the New Energy and Industrial Technology Development Organization (NEDO) [33], and then identified parameters, such as capacity factor and lifetime. Moreover, from the calculated decommissioned capacity, the amount of GFRP/CFRP, which is the major constituent material of blade waste, was calculated for each power generation capacity class. Finally, CO_2 emissions during the processing or recycling of GFRP/CFRP waste generated during the life cycle of wind blades were calculated using the life cycle assessment (LCA) software SimaPro 8 [34].

In addition to current treatment options for blade waste, such as landfilling and incineration, we also considered scenarios that applied mechanical recycling, fluidised bed recycling, and pyrolysis recycling. We focused on the amount of CO_2 emitted from these scenarios. Therefore, we were able to estimate the environmental burden during waste treatment when considering the entire life cycle of wind blades.

Furthermore, the waste generated during the life cycle of wind blades consists of three types: manufacturing, service, and end-of-life wastes [6]. In the manufacturing life cycle stage, the condition that wind blade waste produces defective products was considered. In addition, wind blade waste should be considered during O&M, including regular maintenance, repairs, and blade replacement due to failure [6]. Figure 1 presents the flow of this research and an overview of the life cycle stages of wind blade waste.

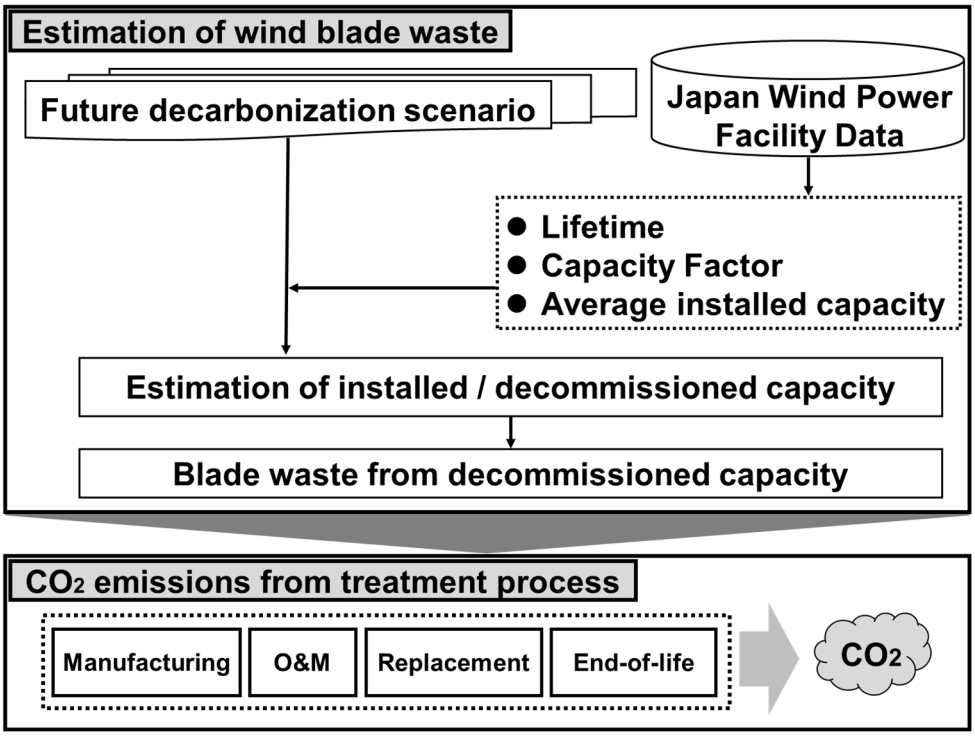

Figure 1. Research flow and life cycle stages of wind blade waste.

2.2. Future Energy Scenario

The target was the 2050 decarbonisation scenario [31] examined using the Asia-Pacific integrated model (AIM), which was developed by the National Institute for Environmental Studies and other organisations in 1990. Four scenarios were envisioned, and the LED scenario [31] adopted in the IPCC special report on 1.5 °C [5,31] was adopted in the current study. The LED scenario was set on the basis of the assumption that a society will transform into one where energy-saving materials can provide high benefits and effectiveness due to changes in living and working styles towards a decarbonised society in 2050 [31]. The AIM model study referenced in this study was the AIM/Enduse model, which is a technology selection framework for policy analysis related to reducing GHG emissions and controlling global air pollution [35]. In particular, AIM/Enduse calculates CO_2 emissions from energy consumption, which are then calculated backward from the consumption of fossil fuels, new fuels (e.g., hydrogen), and electricity in the transportation, household, business, and other sectors, which are the final consumption sectors, as well as the industrial sectors. Figure 2 shows the trends in the total power generation $\sum_p E_{tp}$ from wind energy until 2100 under the LED scenario (AIM) used in this study. From the LED scenario, the target values for total wind power generation in 2030 (onshore: 16 TWh, offshore: 2 TWh) and 2050 (onshore: 190 TWh, offshore: 292 TWh) were obtained. We calculated the value of the total power generation in 2040 from the ratio of the increase in the amount in the Northern Hemisphere between 2030–2040 and 2040–2050 from the LED scenario database [36]. We also defined the growth rate of total power generation in each year on a 10-year basis, similar to the LED scenario data [36], and calculated the total power generation. The growth rate of total power generation from 2020 to 2050 was calculated from the total power generation in 2020, 2030, 2040, and 2050. For the total power generation from 2050 to 2100, we applied the growth rate of total power generation in 10-year units for onshore and offshore wind power generation in the Northern Hemisphere from the LED scenario database [36]. In the LED scenario, the total onshore wind power generation in the Northern Hemisphere is projected to increase through 2100 [36]. From another perspective, offshore wind power generation in the Northern Hemisphere is predicted to decrease after 2050 in the LED scenario, and the amount of power generation will reach zero in 2081 [36]. For total power generation before 2020, we used the past installed capacity [33] and actual values from the electricity survey statistics [23] for onshore wind power. Offshore wind power is still in the early stages of development in Japan [37]; hence, the amount of power generated by offshore wind power before 2020 is assumed as zero. Therefore, offshore wind power was introduced starting in 2021.

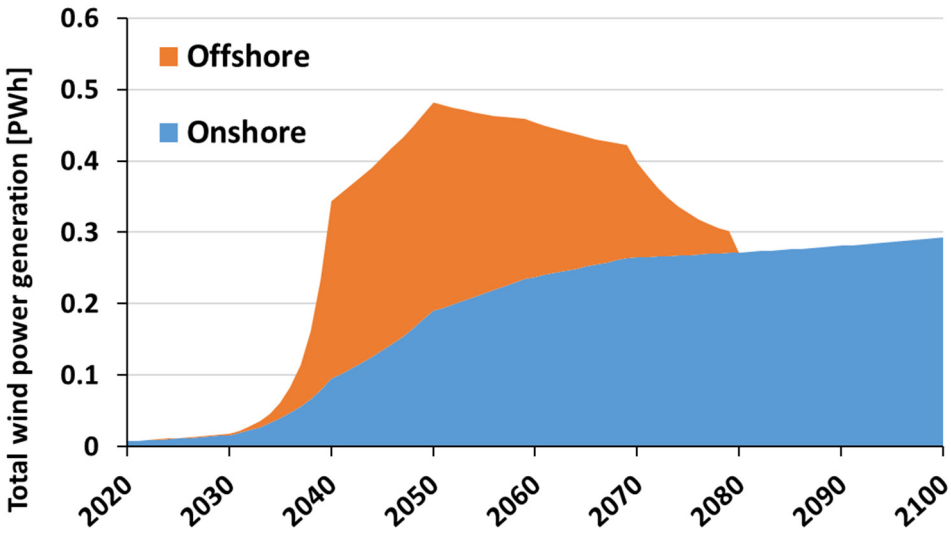

Figure 2. Total wind power generation (Ep) in the LED scenario. Measured values were used for 2018–2020. Data for 2030 and 2050 were taken from the LED scenario. The growth rate of the total power

generation in each year was calculated on a 10-year basis, and that from onshore and offshore wind in the Northern Hemisphere was applied from the LED scenario database [36]. Reproduced with permission from the Asia-Pacific Integrated Model project team, A Trial Calculation of the Realization of a Decarbonized Society in 2050, published online in 2020 [31]. Reproduced with permission from Ministry of Economy, Electric Power Survey Statistics [23]. This figure is based on the LED database jointly hosted by the IIASA Energy and Transitions to New Technologies Programs at https://db1.ene.iiasa.ac.at/LEDDB, accessed on 23 February 2024. The underlying scientific data was published in Nature Energy [38].

2.3. Calculation Model for Wind Blade Waste Amount

To calculate the amount of wind blade waste for each year, we estimated the installed/decommissioned capacity of wind power generation for each year from the LED scenario. Figure 3 shows the relational diagram of the formula for calculating the amount of wind blade waste for each year from the total power generation amount $\sum_p E_{tp}$ for each year from the LED scenario. These details are explained in Sections 2.3.1 and 2.3.2.

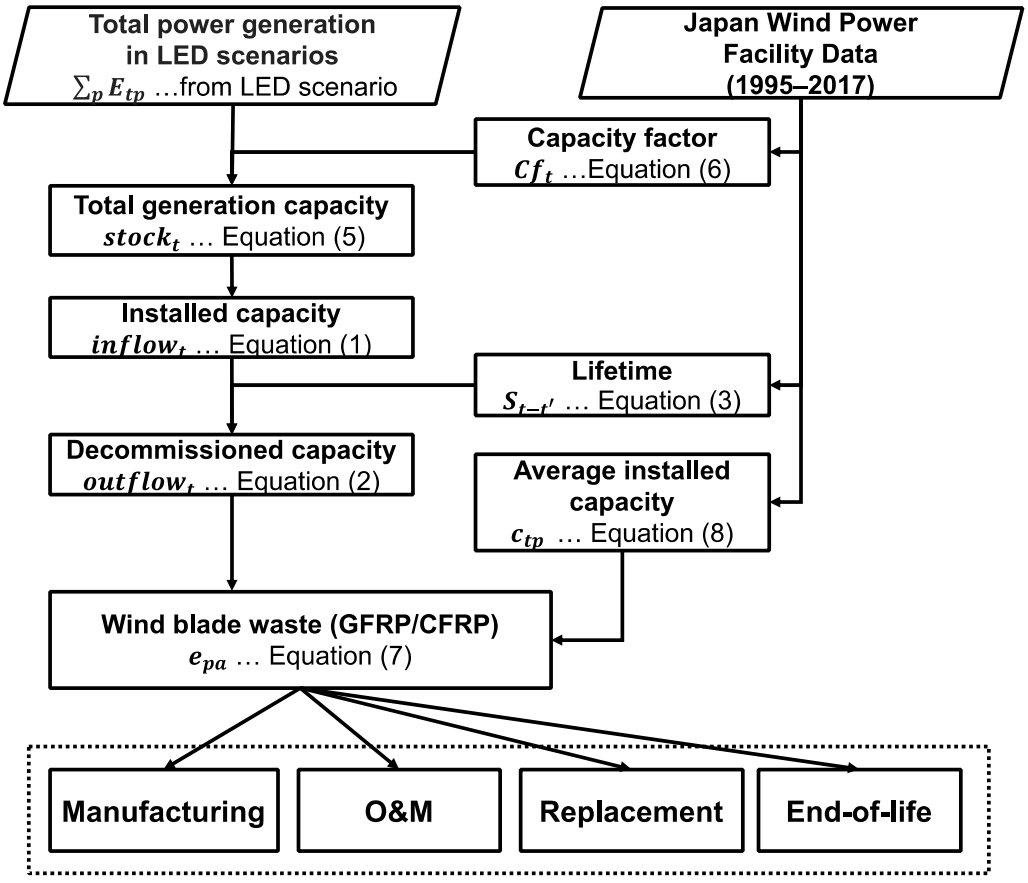

Figure 3. Model diagram of the calculation formula required to estimate the amount of wind blade waste. The decommissioned capacity was calculated from the total power generation of the LED scenario using the capacity factor and lifetime model formula. The wind blade waste installed in year t was calculated from the average installed capacity. The amount of blade waste generated during its life cycle was calculated from the weight of the blade itself.

2.3.1. Calculating Installed/Decommissioned Capacity

On the basis of the total generation capacity (the LED scenario) of onshore and offshore wind power generation until 2100, the installed capacity that will be newly introduced

each year and the decommissioned capacity after the lifetime expires are calculated using Equations (1) and (2) [39].

$$inflow_t = stock_t - stock_{t-1} + outflow_t, \tag{1}$$

$$outflow_t = \sum_{t'=t0}^{t'=t-1} inflow_{t'} \times (1 - S_{t-t'}), \tag{2}$$

$$S_{t-t'} = \frac{\kappa}{\lambda}\left(\frac{t-t'}{\lambda}\right)^{\kappa-1} exp\left\{-\left(\frac{t-t'}{\lambda}\right)^{\kappa}\right\}, \tag{3}$$

Average lifetime (μ) can be calculated from scale parameter (λ) and shape parameter (K).

$$\mu = \lambda \times \Gamma\left(1 + \frac{1}{\kappa}\right), \tag{4}$$

Here, $stock_t$ (Equation (1)) is also shown as follows:

$$\begin{aligned} stock_t &= \sum_p c_{tp}, \\ &= \frac{\sum_p E_{tp} \times 100}{T \times Cf_t}, \end{aligned} \tag{5}$$

$$Cf_t = 0.24 \times year - 461, \tag{6}$$

where

$inflow_t$ = total installed capacity in year t;
$stock_t$ = total generation capacity in year t;
t' = year of installation of power generation equipment;
$outflow_t$ = total decommissioned capacity in year t;
$S_{t-t'}$ = probability of reaching lifetime in year $t - t'$;
K = shape parameter;
λ = scale parameter;
μ = Average lifetime;
c_{tp} = generation capacity of wind farm p in year t [MW];
E_{tp} = power generation of wind farm p in year t [MWh];
T = annual operating hours (365 days × 24 h = 8760 h);
Cf = capacity factor in year t [%].

The installed capacity ($inflow_t$) in year t in Equation (1) means the sum of "newly installed equipment in year t" and "replaced obsolete equipment". By substituting Equation (3) into $S_{t-t'}$ in Equation (2), we calculated the statistical decommissioned capacity based on the lifetime of the installed wind power generation equipment and the equipment introduced in the past. The lifetime of wind power generation equipment can be statistically approximated via the Weibull distribution [39,40], and $S_{t-t'}$ is the lifetime of wind power generation in year $t - t'$ expressed by the Weibull distribution [Equation (3)].

The shape parameters used in the Weibull distribution for wind power indicate the damage rate of the wind turbine [41]. The meaning of the damage rate changes depending on the size of the shape parameter (K) [41]. The shape parameter (K) used in the Weibull distribution is a constant that differs depending on the type of equipment, and 2.0 is generally used for wind power generation [41]. In addition, some studies [39] have been conducted with a shape parameter of 4.07, whilst others have used a shape parameter of 1.73 for power plants that include wind power generation [18]. In the current study, Case 1 was set as 1.73, Case 2 as 2.0, and Case 3 as 4.07, with Case 2 as the base case. Hereafter, Case 1 is referred to as C1, Case 2 as C2, and Case 3 as C3. The lifetime of wind power generation equipment generally lasts around 20–25 years [42–45]. Considering that their lifetimes may depend on the country's climate and regional characteristics, we analysed data on past equipment introduced and discontinued in Japan. In the Weibull

distribution of lifetimes, the average lifetime can generally be expressed in terms of a gamma function [41]. To obtain the scale parameter (λ) that constitutes Equation (3), the shape parameter (K) and average lifetime (μ) were inputted into Equation (4).

We analysed trends in equipment installed in Japan on the basis of the results of wind power generation equipment and installation in the country from 1980 to 2017 provided by the New Energy and Industrial Technology Development Organization (NEDO) [33]. When targeting equipment installed up to 2017 that included "electricity sales business" in its installation usage, we extracted data from 1995 to 2017. The extracted data are explained in Appendix A. From the actual measured data [33] (Figure A1) from 1995 to 2017, the average lifetime of wind power generation equipment in Japan has been trending at 20 years to 25 years. Therefore, the average lifetime was set to 20 years and 25 years in the current study, a scale parameter was created from Equation (4), and the Weibull distribution was created from Equation (3) (Figure A1).

Furthermore, the total generation capacity ($stock_t$) of onshore/offshore wind power in year t used in Equation (1) was $\sum_p c_{tp}$, which was calculated using Equation (5) based on the LED scenario. The total generation capacity ($\sum_p c_{tp}$) in year t was calculated using the capacity factor (Cf_t) in year t, the annual operating time (T), and the power generation amount ($\sum_p E_{tp}$) in the LED scenario (AIM) (Figure 2) [Equation (5)].

The capacity factor of wind power generation in year t (Cf_t) [%] was found to change linearly over time, according to a study in Sweden that investigated the capacity factor of wind turbines at the national level [46]. This factor is calculated from the 20-year capacity factor trend line for the entire Swedish wind energy sector from 1994 to 2014 [46]. The capacity factor is the annual production of wind power divided by the maximum output possible if all turbines operated at full power during the year [46]. Therefore, the capacity factor of the wind turbine used in the current study was assumed to change over time in accordance with a linear function. Furthermore, when the wind industry sector expands in Japan, equipment similar to that in Sweden, where the introduction of wind power generation is progressing, is expected to be introduced in Japan. Equation (6) [46] shows the capacity factor in year t (Cf_t) [%].

2.3.2. Estimation of Wind Blade Waste Amount from Installed/Decommissioned Capacity

The weight of the wind blade itself was calculated from the installed/decommissioned capacity determined in Section 2.3.1. The material weight of the blade body was calculated from the blade mass per power generation capacity calculated for each power generation capacity class (the blade itself was calculated from the installed/decommissioned capacity determined in c_{tp}) per installed unit was also applied to the current study [6]. Table 1 shows that Equation (7) is used for calculating the total weight (e_{pa}) of GFRP/CFRP waste and the parameters for each class [6].

$$e_{pa} = w_p \, c_{tp} \times \frac{\gamma_{tpa}}{100}, \tag{7}$$

where

e_{pa} = amount of GFRP/CFRP (a) blade waste at wind power plant p [t/unit];

w_p = blade weight per MW of power generation capacity [t/MW];

c_{tp} = installed capacity per unit of wind farm p in year t [MW/unit];

γ_{pa} = material-specific assignment parameters in a (GFRP/CFRP) at wind power plant p [%].

Table 1. List of calculation parameters for GFRP/CFRP waste amount by the power generation capacity class *.

Capacity Class *	c_{tp}	w_p	$\gamma_{p \mid tp<2001}$ [%] **		$\gamma_{p \mid tp\geq2001}$ [%] **	
	[MW]	[t/MW]	GFRP	CFRP	GFRP	CFRP
Class 1	$0.0 < c_p < 1.0$	8.43	89.0	0	89.0	0
Class 2	$1.0 \leq c_p < 1.5$	12.37	87.0	0	87.0	0
Class 3	$1.5 \leq c_p < 2.0$	13.34	86.0	0	81.0	27.5
Class 4	$2.0 \leq c_p < 5.0$	13.41	84.0	0	78.5	3.00
Class 5	$5.0 \leq c_p$	12.37	82.0	0	74.5	3.40

* Reproduced with permission from Liu et al., Wind turbine blade waste in 2050; published in 2020 [6]. ** The allocation parameters of GFRP/CFRP are different, depending on whether it was introduced before 2000 or after 2001.

From Equation (7), the average installed capacity (c_{tp}) per unit of wind power generation in year t is calculated using the linear prediction formula of Equation (8) by combining past data [33] and the predicted value [39] of previous research. As a result of linear regression using the measured data from 1995 to 2017 [33] and the future predicted values for 2030 and 2050 [39], the slope was 0.933 and the intercept was 185.78 ($R^2 = 0.92$). For the average installed capacity of wind power, measured data from 1995 to 2017 were used for onshore wind power (Section 2.3.1). For onshore wind power data from 2018 onward, the average installed capacity (c_{tp}) per unit of wind power plant was calculated using Equation (8).

$$c_{tp} = 0.933 \times year - 185.78 \quad (8)$$

Meanwhile, no actual measured values for offshore wind power were found [39], but predicted values based on previous research were available. In the current study, we applied estimates of the average installed capacity of offshore wind for each year until 2100. The average installed capacity in Akita Prefecture in the northern region of Japan, which was selected as a region to promote offshore wind power, was 4.2 MW [47]. Therefore, we assumed a linear increase based on 4.2 MW in 2021, 12 MW in 2030, and 15 MW in 2050 [39,47]. The average installed capacity (c_{tp}) per unit for onshore and offshore wind power will remain constant after 2050 due to the maturity of the wind power industry. In the LED scenario, the growth rate of total wind power generation is projected to stagnate globally after 2050 [36]. This study examines the case in which the wind power industry matures, and the size of wind turbines ceases to increase. Nevertheless, there is a possibility that the average installed capacity will continue to grow after 2050 (Appendix B). Considering the evolution and technological innovation of this industry, wind power generation will possibly become larger even after 2050, and thus, attention must be given to the future of the wind power industry.

Figure 4 shows an image of wind blade waste generation. When the total weight of the wind blade itself was taken as 100%, the amount of waste emitted during the four life cycle stages (Figure 1) defined in this study was expressed as a percentage in accordance with previous research [6]. It was set as a waste emission factor [%] [(waste weight at each life cycle/blade body weight) × 100] (Table 2). At each life cycle stage, waste is discharged in accordance with the specified discharge year (Table 2). Furthermore, at the end-of-life stage, 100% of the blade itself will be discharged as waste [6]. Three cases were set for the manufacturing stage and service stage: Case 1′, Case 2′ (base), and Case 3′ [6]. Values of parameters used in Case 2′ were close to median in various scenarios in previous studies [6]; therefore, it was set as the "basic case" in this study. Hereafter, Case 1′ will be referred to as C1′, Case 2′ (base) as C2′, and Case 3′ as C3′. When calculating the amount of wind blade waste, three cases (C1, C2, and C3) were set for the shape parameter (K) used for the Weibull distribution (lifetime) (Section 2.3.1). We calculated nine different combinations for each.

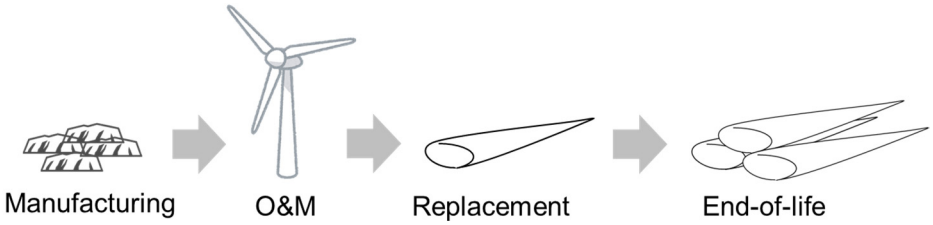

Figure 4. Images of wind blade waste generation. One unit of wind power generation equipment consists of three blades.

Table 2. Blade waste emission factor at each life cycle stage *.

Life Cycle Stage	Discharge Year $t-t'$ [Year]	Case 1′ [%]	Case 2′ (Base Case) [%]	Case 3′ [%]
Manufacturing	0	12.1	17.2	30.4
Service, O&M	5	1.5	2.9	4.6
Service, Replacement	15	2	5	10
End-of-life	$S_{t-t'}$ (Lifetime)	100	100	100

* Reproduced with permission from Liu et al., Wind turbine blade waste in 2050; published in 2020 [6].

2.4. CO_2 Emissions during Recycling or Disposal at Each Life Cycle Stage

In this section, we calculated the CO_2 emissions when recycling or disposing of wind blade waste. Each country has its own characteristics with regard to waste disposal [7,8,15]. In the current study, Japanese data [48] were applied for the proportion of recycling types, whilst European data [10] were applied for the recycling process of wind blade waste for each recycling type. At present, processing methods and proportions of plastic industrial waste in Japan are mechanical recycling (27.4%), chemical recycling (0.25%), thermal recycling (60.8%), and combustion or landfilling (11.6%) [48]. However, given that the GFRP and CFRP considered in this study are waste materials that contained plastic and reinforcing materials, separating the glass and carbon materials from the polymer is necessary when processing them during thermal recycling and chemical recycling [10]. Therefore, the blades (GFRP/CFRP waste) removed from the turbine were cut, crushed, and reduced in weight via a mechanical treatment process (pre-diminishing) [10]. The crushed waste was transported to each recycling type treatment process described above. In particular, (1) mechanical recycling includes milling, (2) chemical recycling includes high-voltage fragmentation and solvolysis, (3) thermal recycling includes pyrolysis and a fluidised bed process, and (4) disposal includes incineration and landfilling (Figure 5).

CO_2 emissions reduced by heat recovery during the treatment process were also calculated. Wind blade waste was assumed to undergo a treatment process during the year it was discharged, and thus, the intermediate storage of wind blade waste was not considered.

In addition, this study did not consider the secondary use of recovered GFRP/CFRP materials. Many studies have assumed that the recovered materials will be supplied to the market again after recycling GFRP/CFRP waste [10–18]; however, some issues exist. GFRP and CFRP are cross-linked, and thus, they cannot be reformed and the economic incentive for recycling is small [19]. Material recovery from mechanical recycling requires significant financial support [7]. Recycling GFRP may have a considerably lower cost–benefit advantage than recycling CFRP [21]. The materials recovered by recycling CFRP are not cost competitive; hence, incineration and landfilling have been suggested to continue as the mainstream [17]. In addition, the strength of GFRP/CFRP decreases due to recycling, and obtaining the strength of the primary materials is difficult through mechanical recycling [16]. Thermal recycling can reduce the strength of recycled glass materials by 50–60%, and even up to 80% [20]. Chemical recycling maintains the strength of the recycled materials to a certain extent compared with other methods [20]; however, it can be costly [21]. Some studies have also considered incineration and landfilling as blade waste treatment

processes [9,18]. For the aforementioned reasons, we assumed in the current study that although the recycling method for GFRP/CFRP has already been socially implemented, the usefulness of secondary materials cannot be established.

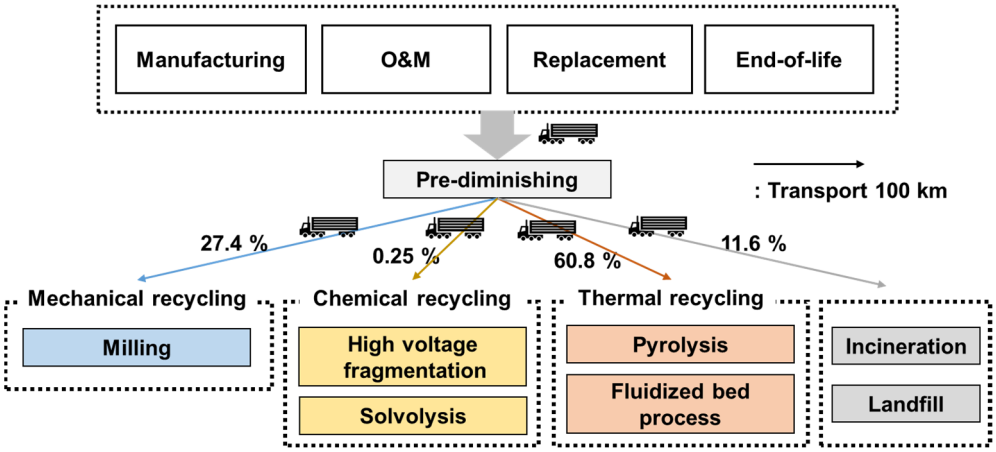

Figure 5. GFRP/CFRP waste treatment process flow. After pre-diminishing, waste is transported 100 km by lorry and assigned to multiple processing steps. The percentage of each treatment process was based on Japan's plastic waste treatment method [48]. Reproduced with permission from Japan Plastic Recycling and Reuse Association, Production, Disposal, Recycling, Treatment and Disposal of Plastic Products in Japan; published online in 2023 [48].

The amount of CO_2 emitted during the transportation of blade waste was also considered between each treatment process. In the current study, we used land lorry transport (market for transport, freight, lorry 16–32 t, EURO5, global [GLO]) from ecoinvent3 [49] in line with previous research [10]. The road distance from the locations where onshore/offshore wind power has been introduced (Akita Prefecture and Hokkaido) to the industrial waste treatment facility was approximately 100 km; thus, the transport distance for blade waste was set at 100 km. Although the transport distance can be variable, we set a constant value considering the geographical conditions in Japan. In some LCA studies, transport distance is also treated as a constant depending on their research areas [7].

Milling is 100% mechanical recycling, and fixed values for incineration and landfilling are determined for disposal. The proportions of chemical recycling and thermal recycling are not known from previous research; therefore, a scenario in which each proportion is equally divided at 50% was used as the base scenario. For sensitivity analysis, we selected the CO_2 lowest scenario (solvolysis for chemical recycling, and fluidised bed process for thermal recycling) as the recycling scenario with the lowest CO_2 emissions and the CO_2 highest scenario (high-voltage fragmentation for chemical recycling, and pyrolysis for thermal recycling) as the recycling scenario with the highest CO_2 emissions (Table 3). Amongst the nine patterns calculated, we multiplied the minimum wind blade waste volume [Mt] and ΣGWP [kg CO_2eq/t] of the lowest scenario (Table 3); the wind blade waste volume of base case [Mt] (Case 2′) and ΣGWP [kg CO_2eq/t] of the base scenario (Table 3); and the maximum value [Mt] and ΣGWP [kg CO_2eq/t] of the highest scenario (Table 3) to calculate three patterns. From the three scenarios, ΣGWP [Mkg CO_2eq/t] was calculated for the treatment of wind blade waste. Table 3 lists the wind blade waste treatment process methods used in the current study and the proportion of individual recycling processes in the total (e.g., high-voltage fragmentation, solvolysis).

The life cycle inventory (LCI) data (ecoinvent3) used for each recycling method are provided in Appendix C. LCI data were taken from ecoinvent3 [49], and Japanese inventory data were used wherever possible. However, inventory data, such as lorry transportation and waste plastics, were only available as world average data (rest of the world [RoW]; GLO) [49], and thus, we used these data. Therefore, the effect on the final CO_2 emission

calculation result is considered extremely small and does not affect the final result. In addition, to calculate CO_2 emissions from the recycling or disposal of blade waste, we used IPCC 2013 GWP 100a [50], which can convert GHG emissions into CO_2 emissions. Although the analysis period can be selected as 20, 50, or 100 years [34,50], we chose 100 years because the analysis period for this study is long. The GWP [kg CO_2eq] for each recycling and treatment process was calculated using the LCA software, SimaPro 8 [34].

Table 3. Percentage and GWP of recycling processes for each scenario.

Treatment Type	Process	Low Scenario	Base Scenario	High Scenario
		[%]	[%]	[%]
Pre-diminishing	Shredder	100	100	100
Transport	Lorry transport	100	100	100
Mechanical	Milling	27.4 *	27.4 *	27.4 *
Chemical	High-voltage fragmentation	0	0.13	0.25
	Solvolysis	0.25	0.13	0
Thermal	Pyrolysis	0	30.40	60.80
	Fluidised bed process	60.80	30.40	0
Disposal	Incineration	3.77 *	3.77 *	3.77 *
	Landfilling	7.79 *	7.79	7.79

* Reproduced with permission from Sommer et al., Steering Sustainable End-of-Life Treatment of Glass and Carbon Fiber Reinforced Plastics Waste from Rotor Blades of Wind Power Plants; published in 2021 [10]. Reproduced with permission from Japan Plastic Recycling and Reuse Association, Production, Disposal, Recycling, Treatment and Disposal of Plastic Products in Japan; published online in 2023 [48].

3. Results and Discussion

3.1. Future Estimates of Installed/Decommissioned Capacity

We calculated the annual installed and decommissioned capacities of wind power generation to calculate the amount of blade waste up to the year 2100. Figure 6 shows annual installed and decommissioned capacities when the average lifetime (μ) is 20 years (Figure 6a) and 25 years (Figure 6b) based on the LED scenario [31] (Section 2.2), which is the energy scenario used in the current study.

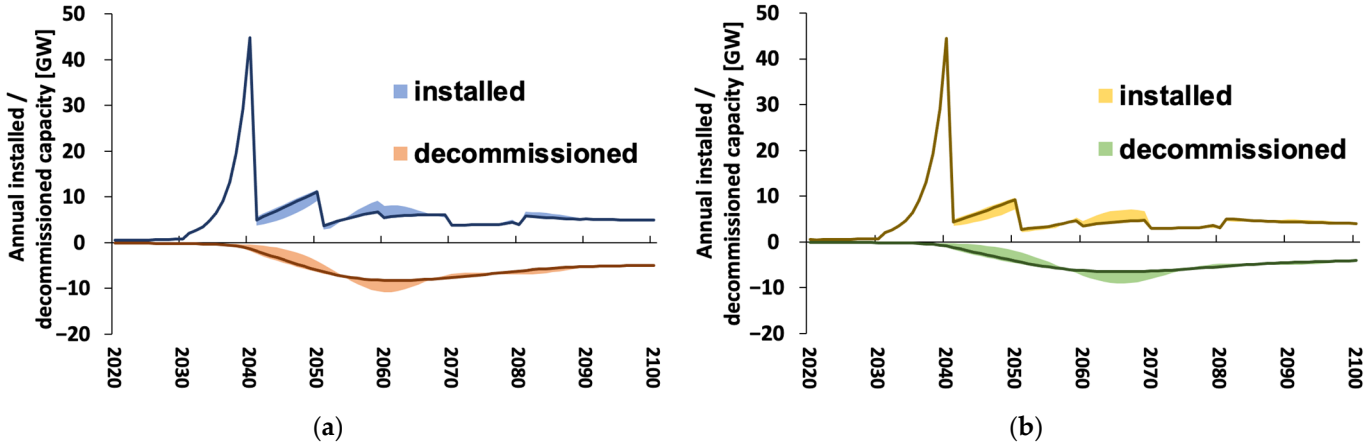

Figure 6. (**a**) Average lifetime (μ) = 20. (**b**) Average lifetime (μ) = 25. Estimation results for installed and decommissioned capacities from 2020 to 2100 in the base case. Decommissioned capacity exhibits the increase as a negative value. The solid line is C2 (K = 2.0). The coloured area indicates the amplitude of variation between C1 (K = 1.73) and C3 (K = 4.07).

When μ = 20 (Figure 6a), annual installed capacity in 2040 will increase by 21.5–21.6 times compared with that in 2031. In the case of μ = 25 (Figure 6b), it will increase by 21.9–22.0 times in 2040 compared with that in 2031. The results show that annual installed capacity will reach its maximum in 2040 for μ = 20 and 25 (K: C2) (Figure 6). Therefore, installing large amounts of wind power generation capacity, particularly between 2031 and 2040, is necessary to increase the total amount of wind power generation by 2050 based on the low-carbon LED scenario [31]. In addition, annual installed capacity in 2041 will decrease by 0.084–0.12 times compared with that in 2040 when μ = 20 (Figure 6a). When μ = 25, it will decrease by 0.080–0.11 times compared with that in 2040 (Figure 6b). The reason is the change in the growth rate of total offshore wind power generation on a 10-year basis in the LED scenario [31] (Section 2.2). The growth rate of total offshore wind power generation in 2030–2040 will be the largest, whereas that in 2040–2050 will be relatively small. The installed offshore wind capacity for each year is the sum of installed capacity to increase total offshore wind power generation (A) and installed capacity to replace retired facilities (B). In other words, the growth rate of the total offshore wind power generation will decrease from 62.0% to 1.6% in 2040 and 2041. Hence, the results reflect the decrease in installed capacity (A) owing to the increase in the total power generation.

Furthermore, from 2051 onwards, the annual installed capacity changes on a 10-year basis. The reason is a decrease in the total amount of electricity generated by offshore wind. In the LED scenario [36], offshore wind power is projected to decline after 2050. Figure 6 depicts the changes in the annual installed capacity of offshore wind power generation. However, the growth rate of Japan's total power generation needs to be applied to the LED scenario [36] to determine the power generation needed over a longer period to account for the impact of wind blade waste.

Meanwhile, the maximum value of decommissioned capacity will be 8.3 GW in 2062 (Figure 6a) and 6.5 GW in 2065 (Figure 6b) when K is the base case (C2) and μ = 20 and 25, respectively. When the shape parameter (K) of the Weibull distribution is C1 and C3, the difference between the maximum and minimum decommissioned capacities is 2.6 and 2.8 GW when μ = 20 and 25, respectively (Figure 6). Furthermore, decommissioned capacity is estimated to increase from around 2031 to 2040 for μ = 20 and 25, because facilities that will be introduced in large numbers between 2060 and 2065 will have reached their respective lifetime and be decommissioned.

3.2. Results for Average Installed Capacity of Wind Power

We calculated the average installed capacities to calculate the amount of blade waste up to the year 2100. In addition to the installed capacity in year t, the average installed capacity in year t (c_{tp}) is required when calculating the amount of wind blade waste. Figure 7 presents the results of setting the average installed capacity (c_{tp}) in year t. Onshore wind power will increase linearly to 3.6 MW in 2030 and 5.5 MW in 2050. This result is considered to exhibit validity in the created model because the deviation from the future goals of a previous study [39] (4 MW in 2030, 5 MW in 2050) has become smaller.

Meanwhile, offshore wind power will increase by 7.8 MW from 2021 to 2030 and by 3 MW from 2031 to 2050 when the situation from a previous study [39] to achieve the target of 12 MW in 2030 and 15 MW in 2050 is applied. The increase rate of the average installed capacity for offshore wind power between 2031 and 2050 is smaller than that between 2021 and 2030 but larger than that for onshore wind power.

For the average installed capacity of onshore wind power, the measured values from 1995 to 2017 were used, but linear projections of the measured values were used from 2018 to 2050 (Section 2.3) due to technological innovations that increased the size of wind turbines and blades [37]. The measured value was also confirmed to increase linearly from 1995 to 2017, and even after, the average installed capacity per unit has been confirmed to increase every year from actual implementation cases in Denmark [39].

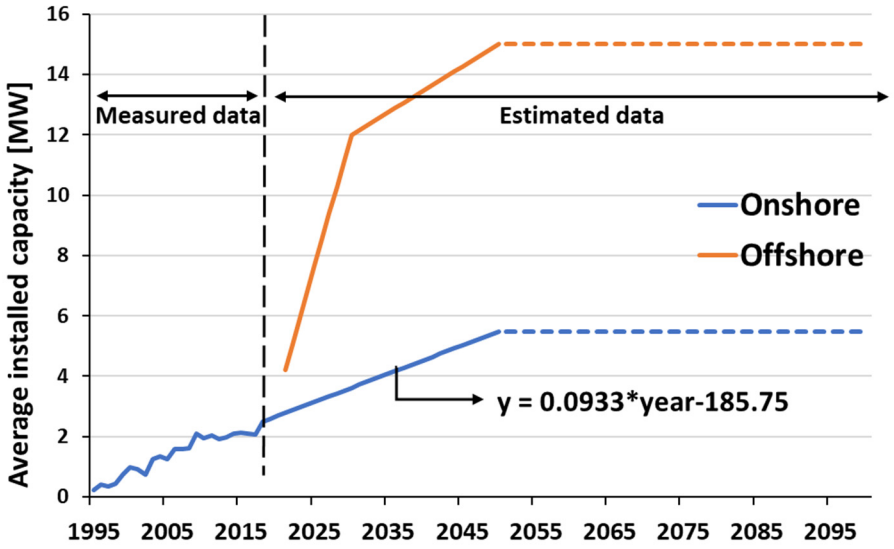

Figure 7. Trends and linear approximation of average installed capacity from 1995 to 2017. Measured data from Japan [33] were used for onshore wind power from 1995 to 2017. The average installed capacity of onshore wind power from 2018 to 2050 is a linear prediction based on previous data [33]. Offshore wind power was scheduled to be introduced in 2021, and thus, only estimated data are shown.

Meanwhile, considering the fact that the trend in onshore wind power is likely to increase linearly based on actual measurements, offshore wind power will need to increase at an even faster rate than onshore wind power to achieve the 2050 target. In reality, however, the average installed capacity of offshore wind turbines tends to be larger than that of onshore wind turbines, because the installation cost of offshore wind power is higher than that of onshore wind power, and increasing the amount of power generated per unit is important [18]. In fact, offshore wind power generation with a power generation capacity of 450 kW was first introduced in the UK in 1991, but it has now been replaced by offshore wind power generation with a power generation capacity of 5 MW or higher, mostly in Europe [37]. In Japan, offshore wind power is also predicted to become larger than onshore wind power due to the aforementioned reasons [37]. Furthermore, when comparing the slope of the linear increase in offshore wind power between 2021–2030 (0.78) and 2031–2050 (0.14), the latter is slower. However, a target value [31] has been set for the installed capacity of offshore wind power in 2030, and thus, Japan is assumed to advance large-scale offshore wind power generation rapidly by that year. A target value has also been set for 2050 [31], but if the target value for 2030 [31] is achieved, then the increase in average installed capacity from 2031 to 2050 will be slower than it was until 2030.

This trend in onshore and offshore wind power is predicted to continue until 2050 on the basis of the Paris Agreement [4]. Therefore, this study assumes that a linear increase will occur every year until 2050, and after the goal is achieved in 2050, the increase will be less pronounced than that before 2050. Accordingly, this study will remain stable, resulting in the transition shown in Figure 7.

However, considering the evolution and technological innovation in the wind industry even after 2050, wind turbines will possibly become larger in onshore and offshore wind power, and thus, attention should be given to the future wind industry.

3.3. Estimation Results for the Amount of Wind Blade Waste

We calculated the amount of blade waste until the year 2100 to calculate the expected total CO_2 emissions during the waste treatment process by that time. Figure 8 shows the matrix of nine patterns calculated in this study. Figure 9 presents the results of estimating the amount of wind blade waste from the calculated installed/decommissioned capacities (Section 3.1) until 2100.

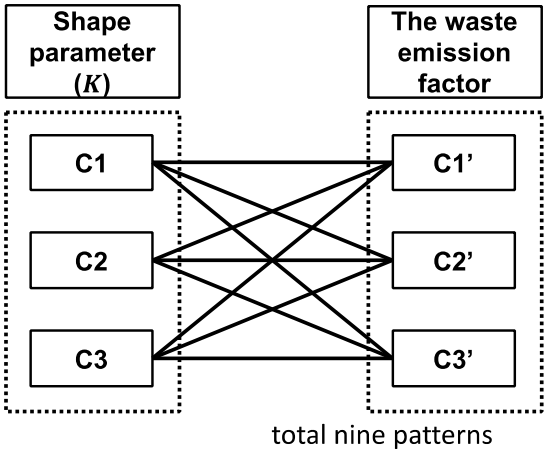

Figure 8. Matrix of nine patterns considered when calculating blade waste volume.

In the base case for μ = 20 and 25, the amount of wind blade waste will start to increase rapidly in 2040 and decrease around 2060.

In the case of μ = 20 (Figure 9a), wind blade waste is estimated to reach a maximum of 0.17 Mt in 2061 in the base case, which is 3.4 times higher than that in 2021, when wind blades were first introduced. In the case of μ = 25 (Figure 9b), the maximum value is 0.15 Mt in 2065 in the base case, which is also estimated to be 2.9 times as much as that in 2021. In addition, for μ = 20 and 25, the amount of waste from 2070 to 2100 will decrease within the range of approximately 0.02 Mt until 2100. Therefore, on the basis of the calculations of the nine patterns considered in this study, the range of possible values after 2070 is ±12.3–18.3% when using the base case as the standard.

As mentioned above, when comparing μ = 20 and 25, differences are found in the amount of wind blade waste compared with the base case and in the years when the difference is narrowed down. The reason for such result is that the nine patterns (Figure 8) are calculated on the basis of the combination of the shape parameter (K) and the waste emission factor (Table 2).

Compared with the base case, C3 × C3′ is significantly different (Figure 9). When μ = 20, the amount of waste in C3 × C3′ remains small compared with that in the base case from around 2040, but it crosses with the base case in 2053, and reaches the maximum value amongst all the cases at around 2060. Similarly, in the case of C3 × C1′, the amount of waste remains small compared with that of the base case from around 2040, but it crosses with the base case in 2055, and reaches the minimum value among all the cases at around 2073. In addition, a slight crossing occurs among the other cases apart from C3. For example, C1 × C3′ crosses not only C3 × C3′ but also C2 × C3′. Amongst the calculation results of the nine patterns, the common feature of the cases that have changed significantly compared with the base case is C3 (K = 4.07), because the shape parameter (K) indicates the damage rate of the equipment. A delay in the timing of decommissioning equipment occurs for C3 (K = 4.07) compared with those for C1 (K = 1.73) and C2 (K = 2.0). Therefore, waves exist in the amount of waste generated, and the peak amount of waste occurs in C3 after 6 years, lagging behind the other cases. By contrast, C1 × C3′ follows a trend parallel to that of the base case from 2030 to 2053 and continues to take the maximum value. Furthermore, C2 × C1′ takes a slightly lower value than the base case, but the fluctuation pattern is nearly the same as that of the base case, because the difference in decommissioned frequency caused by the value of K used in C1 (K = 1.73) and C2 (K = 2.0) is small (Figure 9). When the difference in decommissioned frequency is small, the waste amount curve exhibits a similar shape. Although the curve may go up or down depending on C1′, C2′, and C3′, it is generally parallel to that of the base case.

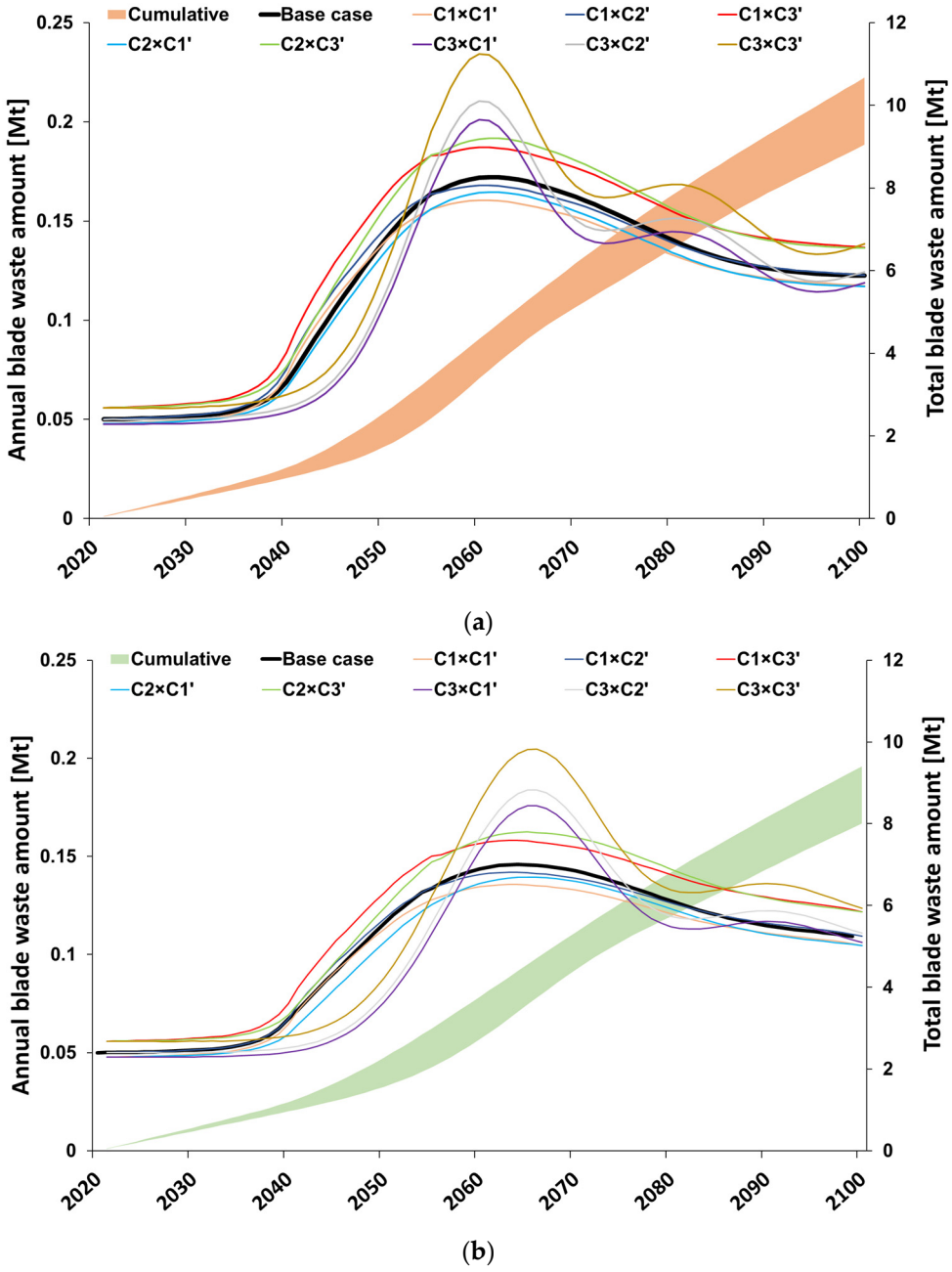

Figure 9. Results of wind blade waste amount in the base case. (**a**) case where μ = 20; (**b**) case where μ = 25. The left axis shows the amount of waste in each year (line graph). The right axis shows the cumulative amount of waste (coloured area). The base case is presented as a solid line to reflect the difference in the lifetime shape parameter (K) (Section 2.3.1) and the waste emission factor (Section 2.3.2). Furthermore, the widths of the minimum and maximum values amongst the nine calculated patterns are presented as coloured areas in Figure 9.

Furthermore, the decommissioned capacity of wind power generation (Figure 6) and the amount of wind blade waste do not necessarily correspond. For example, the maximum value of the decommissioned capacity of wind power generation in the base case will be reached in 2062 (μ = 20) and 2065 (μ = 25) (Figure 6), but the maximum value of wind blade waste in the base case will be reached in 2061 (μ = 20) and 2065 (μ = 25) (Figure 9). The reason for such a result is as follows. In this study, the amount of wind blade waste also includes the amount of waste discarded in each life cycle stage (manufacturing, service, and maximum end-of-life stages). For example, in years when the amount of waste from

the manufacturing and service stages increases significantly, the total amount of waste may increase even if the amount of waste from the end-of-life stage has decreased compared with that in the previous year. In such years, the evolution of wind blade waste volume will not necessarily correspond to the evolution of decommissioned capacity.

With regard to the total blade waste amount, the possible range from 2020 to 2100 will continue to expand. Finally, the difference between the maximum and minimum total blade waste amount will be 16.2 Mt (μ = 20) and 13.9 Mt (μ = 25).

We also confirm the relationship between K and μ from Figure 10. In the case of C3 (K = 4.07), μ takes a value of 20 at the peak of the decommissioned frequency, and we can confirm that the relationship between K and μ is relevant. For C1 and C2, a difference exists between average lifetime (μ) and the peak timing of decommissioning, but no huge difference exists between them when μ = 20. Therefore, the relationship between K and μ is also considered valid for C1 and C2. The same applies to μ = 25.

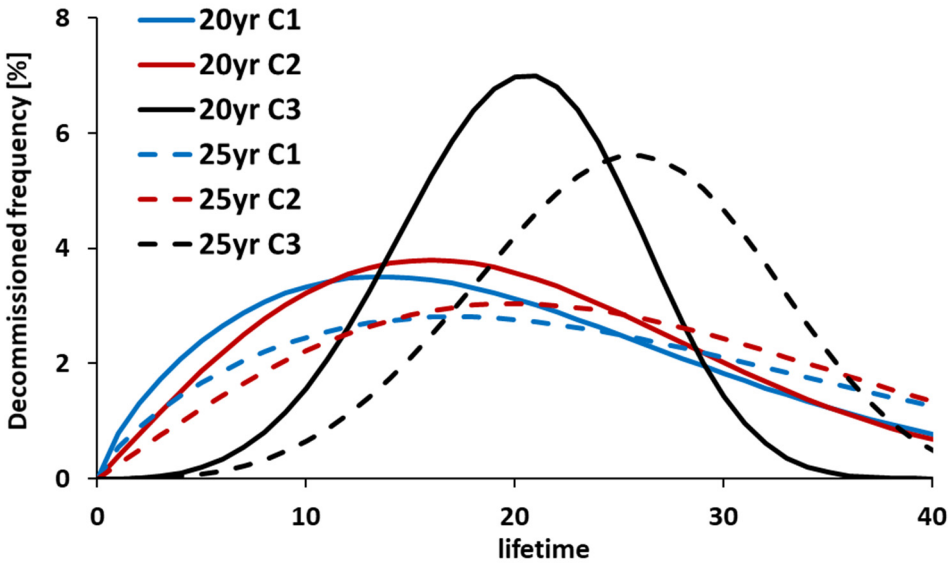

Figure 10. Weibull distribution, lifetime (μ) = 20 years and 25 years of wind power generation equipment. C1 is K = 1.73. C2 is K = 2.0. C3 is K = 4.07. μ = 20 is a solid line, and μ = 25 is a dotted line. In C1 and C2, the decommissioned frequency of the wind power generation equipment reaches its peak earlier than μ, but the difference between them is small.

Furthermore, for μ = 20 and 25, the maximum values are larger around 2055 to 2070 and calculated to be 0.23 Mt and 0.20 Mt, respectively. The amount of wind blade waste must not exceed the waste treatment capacity in Japan. Therefore, when comparing the amount of wind blade waste with the "total amount of industrial waste in the electricity industry in 2020" (10.7 Mt/year) [51], the value is 2.1% (μ = 20) and 1.9% (μ = 25), respectively (Figure 9). Consequently, the calculated waste from wind blades can be processed with the waste treatment capacity in Japan. In addition, the GFRP/CFRP waste emission factors for each blade life cycle used in this study are based on global trends. Therefore, differences may possibly occur when they are used in Japan, and thus, closely examining them is necessary as the wind power generation industry develops in Japan.

3.4. Results of CO_2 Emissions during the Treatment Process of GFRP/CFRP Waste

The CO_2 emitted during the treatment process was calculated from the calculated amount of GFRP/CFRP waste from wind blades. The considered treatment processes were mechanical recycling, chemical recycling, thermal recycling, incineration (no energy recovered), and landfilling (Table 3). Table 4 presents the GWP for three scenarios: the CO_2 lowest scenario with minimum GWP, the base scenario that is set as the general, and the CO_2 highest scenario with maximum GWP (Section 2.4).

Table 4. GWP unit in the treatment process per ton of wind blade waste and GWP unit in the three scenarios **.

Treatment Type	Process	GWP [kg CO_2eq/t]			
		Unit	CO_2 Lowest Scenario *	Base Scenario *	CO_2 Highest Scenario *
Pre-diminishing	Shredder	16.88	16.88	16.08	16.08
Transport	Lorry transport	17.10	17.10	17.10	17.10
Mechanical	Milling	47.52	13.01	13.01	13.01
Chemical	High-voltage fragmentation	10,560	0	13.27	26.53
	Solvolysis	4363	10.96	5.48	0
Thermal	Pyrolysis	3803.18	0	1156.24	2312.48
	Fluidised bed process	384.62	233.86	116.93	0
Disposal	Incineration	329	12.40	12.40	12.40
	Landfilling	14.2	1.106	1.106	1.106
ΣGWP [kg CO_2eq/t]			305.33	1352.42	2399.52

* The GWP for each scenario is the GWP of each processing step multiplied by its ratio. ** Reproduced with permission from Sommer et al., Steering Sustainable End-of-Life Treatment of Glass and Carbon Fiber Reinforced Plastics Waste from Rotor Blades of Wind Power Plants; published by in 2021 [10]. Reproduced with permission from Japan Plastic Recycling and Reuse Association, Production, Disposal, Recycling, Treatment and Disposal of Plastic Products in Japan; published online in 2023 [48].

From Section 2.4, Figure 11 presents the calculation results of GWP in the wind blade waste treatment process for each year.

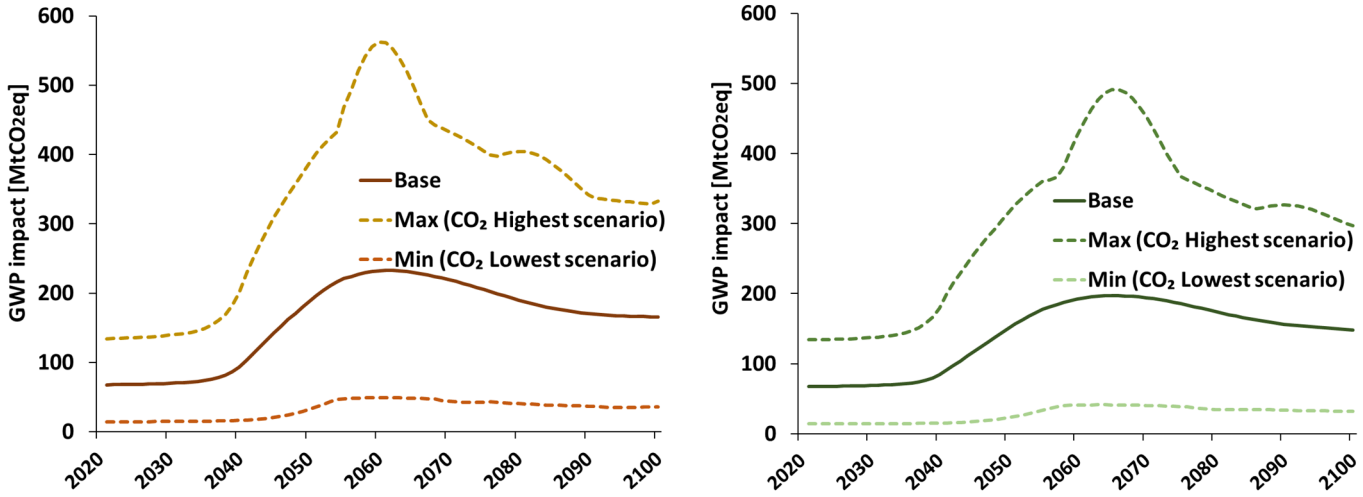

Figure 11. (**a**) Average lifetime (μ) = 20. (**b**) Average lifetime (μ) = 25. GWP wind blades in the treatment process per ton of wind blade waste. Min is the value obtained by multiplying the minimum amount of waste (Figure 9) by the GWP intensity of the CO_2 lowest scenario. Similarly, Base is the value obtained by multiplying the amount of waste in the base case (Figure 9) by the basic unit of GWP in the base scenario, and Max is the value obtained by multiplying the maximum value of waste amount (Figure 9) by the GWP intensity of the CO_2 highest scenario.

Focusing on the base case (Figure 11), when μ = 20, GWP will reach its maximum value (232.9 $MtCO_2$eq) in 2061 and then decrease. At μ = 25, it will reach its maximum value (197.3 $MtCO_2$eq) in 2065 and then decrease. The difference between the years when the maximum value of μ = 20 and 25 is reached is 4 years, and thus, the setting of lifetime (μ) is generally reflected in the results presented in Figure 11. In μ = 20 and 25, Min and

Max exhibit a large deviation from the base. When μ = 20, the maximum value of the base is 232.9 $MtCO_2eq$ in 2061, but the maximum value of Max is 562.0 $MtCO_2eq$ in 2060, which is 2.5 times the base value. The maximum value of Max for μ = 20 will be reached 1 years earlier than the maximum value of the base. Furthermore, Max decreases by approximately 229.6 $MtCO_2eq$ to 2100 after reaching its maximum value. Similarly, when μ = 25, the maximum value of the base is 197.3 $MtCO_2eq$ in 2065, but the maximum value of Max is 491.0 $MtCO_2eq$ in 2066, which is 2.5 times the base value. The maximum value of Max at μ = 25 will be reached 1 years later than the maximum value of the base. After reaching its maximum value, Max decreases by approximately 194.3 $MtCO_2eq$ to 2100.

If wind power generation were to replace thermal power generation, then the GWP that could be reduced by replacing thermal power generation with wind power generation was 13.8 $GtCO_2$, which was calculated from the cumulative total amount of wind power generation in 2021–2100 (23,266.7 TWh, Figure 2) and the CO_2 emission coefficient of thermal power generation in Japan (0.59 $MgCO_2$/TWh) [23,52]. From the results of this study, the GWP of the wind blade waste treatment process until 2100 is 11.4–12.9 $GtCO_2eq$. Therefore, even if the GWP of thermal power generation decreases due to wind power generation, the GWP of the wind blade waste treatment process will account for 82.5–93.6% of the GWP decrease. This study reveals for the first time that the amount of CO_2 emissions contributed by the process of treating wind blade waste is too large to be disregarded.

In addition, the total GHG emissions in Japan expected in 2050 in the LED scenario are approximately 235 $MtCO_2eq$ [31], the CO_2 emissions from wind blade waste (150.2–188.3 $MtCO_2eq$) in the base case approximately account for 63.9–80.1%. We considered two other reasons for the increasing proportion of CO_2 from wind blade waste in the overall total. Firstly, the amount of plastic waste will decrease by 2050 [31]. Secondly, the CO_2 emitted from wind blade waste is converted into pure CO_2 emissions, while the LED scenario presumes that 50% of plastic raw materials should originate from biomass in 2050 [31].

That is, waste from renewable energy equipment, such as wind blades, which were introduced to reduce CO_2 emissions will account for half of the total GWP during waste processing in 2050. Therefore, several issues [7,17,19–21], such as the quality and economic efficiency of secondary materials, must be urgently resolved to achieve low carbonisation.

4. Conclusions

This study quantitatively estimated the amount of CO_2 emissions during the processing of waste generated in each life cycle of wind blades (from manufacture to disposal) when mass-introducing onshore/offshore wind power toward low carbonisation while considering recycling or treatment processes used in Europe [10–13,53]. When recycling wind blade waste, the strength of GFRP/CFRP is reduced and the cost of recycling is increased, and thus, the secondary use of materials has not actually progressed. In this study, calculations were performed on the assumption that although the recycling method for GFRP/CFRP in wind blades has been socially implemented, the usefulness of secondary materials cannot be established.

We calculated the installed/decommissioned capacity of wind power generation in Japan until 2100 by considering the LED scenario (AIM). The life cycle of wind blades was divided into the following stages: manufacturing, service (O&M, replacement), and end-of-life, by considering European recycling or treatment processes. The total amount of blade waste by 2100 was calculated. When the average lifetime (μ) is 20–25 years, the installed capacity will sharply increase from 2031 to 2040 (21.5–22.0 times), reaching its maximum value in 2040. However, installed capacity will decrease sharply from 2040 to 2041 (0.084–0.12 times) and remain stable from around 2060. Meanwhile, when the average lifetime (μ) is 20–25 years, decommissioned capacity will gradually increase and reach its maximum value from around 2030 to 2065, and then it will decrease thereafter. To achieve carbon neutrality in 2050, rapidly introducing a large amount of wind power generation from 2031 is necessary. In particular, offshore wind power is predicted to expand or wind turbines will become larger than those used in onshore wind power.

Nine calculations were performed by combining three cases of parameter (K) representing the damage rate of wind power generation and three cases of the wind blade waste emission factor at each life cycle stage. The base case, in which values that were intermediate for both parameters were chosen, shows an exponential increase until 2065 and then a decrease. Meanwhile, in the two cases that combine the parameters (K = 4.07) in which wind blades are less likely to be damaged, the value will be smaller than that of the base case after 2030. After that, however, one will cross the base case in 2053 and the other in 2055, and then reach the maximum value in all the cases in 2060 and the minimum value in all the cases in 2073. On the basis of the 2020–2100 LED scenario (AIM) [31], the amount of wind power blade waste was calculated, and the maximum value was 0.15–0.17 Mt.

At present, the options for processing wind blade waste are landfilling and incineration. However, even when recycling is considered, the GWP of wind blade waste treatment process in 2050 (150.2–188.3 $MtCO_2eq$) remains extremely large, accounting for approximately 63.9–80.1% of total GHG emissions in 2050 under the LED scenario (approximately 235 $MtCO_2eq$). Moreover, the cumulative GWP of the wind blade waste treatment process until 2100 is 11.4–12.9 $GtCO_2eq$. Even when thermal power generation was replaced with wind power generation, the GWP of the wind blade waste treatment process accounted for 82.5–93.6% of the GWP reduction due to the substitution. Therefore, this study revealed for the first time that the amount of CO_2 emissions contributed by the wind blade waste treatment process is too large to be disregarded. However, the results of this study do not consider the environmental benefits of secondary use, reflecting the current situation where secondary use is difficult to implement owing to the reduced strength and low economic value of recycled materials during recycling. However, as technology develops in the future, where strength is maintained and costs decrease, the secondary use of recovered materials may become widespread. In this case, the calculated GWP during blade waste processing would be based on the fact that primary materials would be reduced through the secondary use of recovered materials, and CO_2 emitted during this process would be reduced.

Accordingly, several issues, such as the quality and economic efficiency of secondary materials [7,17,19–21], must be urgently resolved to realise a low-carbon society.

In this study, predictions were made in accordance with the LED scenario [31], but the amount of power generation equipment that can be installed in 1 year is considered to be limited by the population involved in the wind power generation sector, costs, and construction period. Therefore, future work is expected to incorporate these constraints into the model and examine them closely.

Author Contributions: Conceptualisation, S.N., L.I. and A.T.; methodology, S.N., L.I. and A.T.; validation, S.N., L.I. and A.T.; formal analysis, S.N. and L.I.; investigation, S.N.; resources, L.I.; data curation, S.N. and L.I.; writing—original draft preparation, S.N.; writing—review and editing, L.I., T.N. and A.T.; visualisation, S.N.; supervision, L.I. and A.T.; project administration, L.I.; funding acquisition, L.I. All authors have read and agreed to the published version of the manuscript.

Funding: This research was performed by FY2022-2023 Ministry of Economy, Trade, and Industry Chemical Substance Safety Measures "Chemical Substance Management Advancement Promotion Project in Collaboration with Universities and Public Research Institutions" with an operating expenses grant (20220425 zaisei No.4; 20230512 zaisei No.2) and Management expense grants of Osaka University.

Institutional Review Board Statement: Not applicable.

Informed Consent Statement: Not applicable.

Data Availability Statement: Data are contained within the article.

Acknowledgments: The authors acknowledge the Ministry of Economy, Trade, and Industry for providing funding during the course of this research.

Conflicts of Interest: The authors declare no conflicts of interest. The funders had no role in the design of the study; in the collection, analyses, or interpretation of data; in the writing of the manuscript; or in the decision to publish the results.

Appendix A. Wind Power Generation Facilities Introduced between 1995 and 2017

Among the wind power generation facilities introduced between 1995 and 2017, we extracted those whose purpose was to sell electricity and calculated the survival rate of wind power generation facilities. From Equations (1) and (2), the actual measured values of the Weibull distribution, residual rate, and introduced/decommissioned capacity for a lifetime of 20–25 years are shown in Figure A1. From Figure A1, the lifetime of wind power generation equipment in Japan also changes at approximately 20–25 years. Therefore, the lifetime used in this study was 20–25 years.

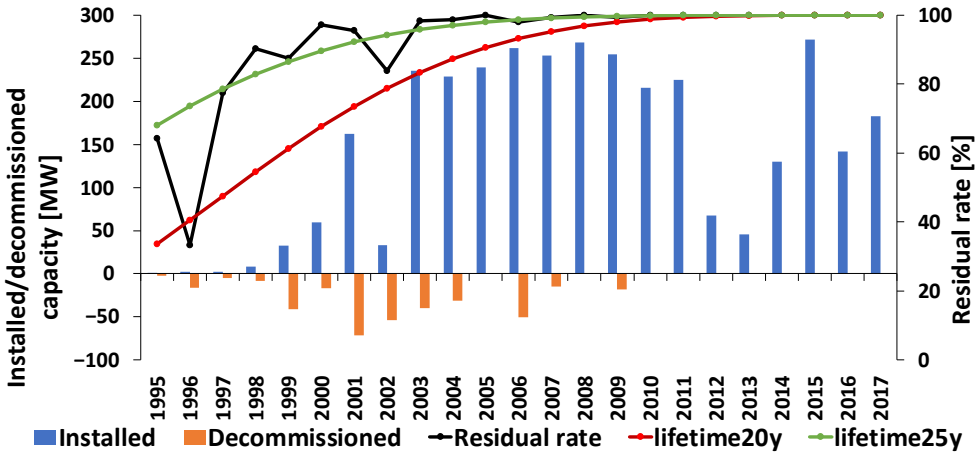

Figure A1. Installed/decommissioned capacity and residual rate of wind power generation from 1995 to 2017, and Weibull distribution of lifetime 20–25 years. The left axis shows installed/decommissioned capacity (solid line). The right axis shows the residual rate (line graph).

Appendix B

In this study, it was assumed that the average installed capacity of wind power generation would stop growing after 2050 as the wind power industry matures. However, it is possible that it will continue to grow even after 2050. Figure A2 shows the case where average installed capacity continues to grow after 2050. In this case, the average installed capacity will increase linearly until 2100, reaching 10.2 MW for onshore wind power generation and 22.5 MW for offshore wind power generation in 2100.

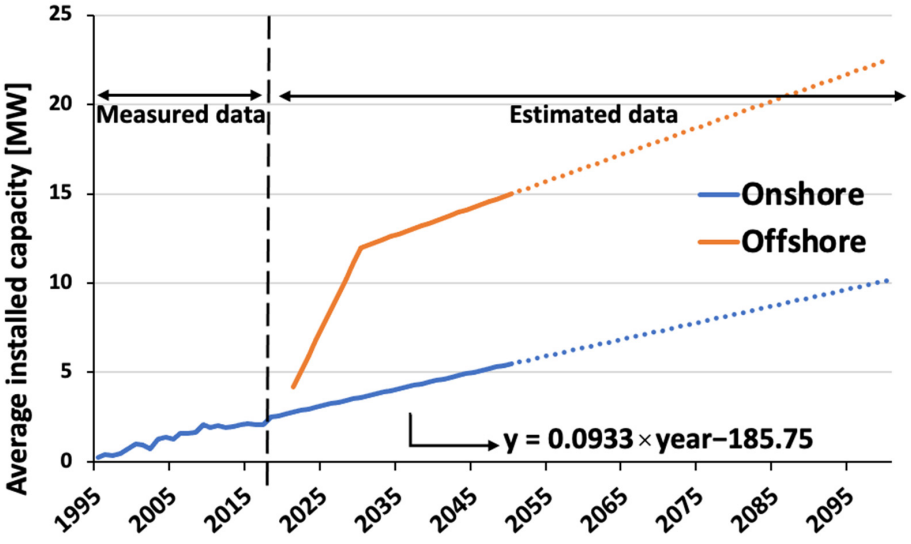

Figure A2. Trends and linear approximation of average installed capacity from 1995 to 2100. Measured data from Japan [33] were used for onshore wind power from 1995 to 2017. The average installed capacity

of onshore wind power from 2018 to 2050 is a linear prediction based on previous data [33]. Offshore wind power was scheduled to be introduced in 2021, and thus, only estimated data are shown. This shows the case where average installed capacity continues to grow after 2050.

Appendix C

In this study, treatment options for GFRP/CFRP waste from the LCI dataset ecoinvent3 were characterised.

Appendix C.1. Pre-Diminishing

Shredding is an essential process before GFRP/CFRP recycling. This process is applied as a preliminary step to all processes. In this process, the wind turbine blade is cut or crushed by a shredder. Table A1 provides the machines used in this phase and their energy consumption. From the LCI data ecoinvent3 [49], the GWP of electric energy (medium voltage) in Japan is 0.634 kg CO_2eq/kWh [49], and thus, the CO_2 emissions in this process were set to 16.88 kg CO_2eq/t.

Table A1. LCI data at pre-diminishing *.

Process	Machine	Consumption [kWh/t]	GWP [kg CO_2eq]
Single-shaft shredder	Vecoplan VAZ 2000	9.88	6.26
Cross-flow shredder	Andriz QZ 2000	16.75	10.62

* Reproduced with permission from Sommer et al., Steering Sustainable End-of-Life Treatment of Glass and Carbon Fiber Reinforced Plastics Waste from Rotor Blades of Wind Power Plants; published in 2021 [10]. Reproduced with permission from the ecoinvent Association [49].

Appendix C.2. Milling (Mechanical Recycling)

In this recycling method, processing is performed using a cutting machine called milling. Here, the materials are crushed and broadly classified into fibres and resins [13]. The energy consumption in the grinding process is 270 MJ/t [13]. The data used are provided in Table A2. From ecoinvent3, the GWP of electric energy (medium voltage) in Japan is 0.176 kg CO_2eq/MJ [49], and thus, the GWP of this recycling method was set to 47.52 kg CO_2eq/t.

Table A2. Ecoinvent3 data at milling *.

Process/Material	Data	Consumption [MJ/t]	GWP [kg CO_2eq/t]
Electricity	Market for electricity, medium voltage | JP	270	47.52

* Reproduced with permission from Sommer et al., Steering Sustainable End-of-Life Treatment of Glass and Carbon Fiber Reinforced Plastics Waste from Rotor Blades of Wind Power Plants; published in 2021 [10]. Reproduced with permission from Howarth et al., Energy intensity and environmental analysis of mechanical recycling of carbon fibre composite; published in 2014 [13]. Reproduced with permission from the ecoinvent Association [49].

Appendix C.3. High-Voltage Fragmentation (Chemical Recycling)

Chemical recycling that uses high-voltage fragmentation is a recycling method that separates fibre reinforcement from the epoxy resin contained in wind blades. Separated epoxy resins and fibres may be supplied to the recycling market as secondary materials. However, this scenario was not considered in this study. In this study, we focused on the energy demand required to generate high-voltage electrical pulses, which was found to consume 60,000 MJ of electricity per 1 t of waste [12]. From ecoinvent3 [49], the GWP of electric energy (medium voltage) in Japan is 0.176 kg CO_2eq/MJ [49], and thus, the GWP of this recycling process is 10,560 kg CO_2eq/t. Inventory data are provided in Table A3.

Table A3. Ecoinvent3 data at high-voltage fragmentation *.

Process/Material	Data	Consumption [MJ/t]	GWP [kg CO_2eq/t]
Electricity	Market for electricity, medium voltage | JP	60,000	10,560

* Reproduced with permission from Sommer et al., Steering Sustainable End-of-Life Treatment of Glass and Carbon Fiber Reinforced Plastics Waste from Rotor Blades of Wind Power Plants; published in 2021 [10]. Reproduced with permission from Mativenga et al., High voltage fragmentation and mechanical recycling of glass fibre thermoset composite; published in 2016 [12]. Reproduced with permission from the ecoinvent Association [49].

Appendix C.4. Solvolysis (Chemical Recycling)

Chemical recycling via solvolysis uses high/low temperature and pressure to separate the fibre reinforcement from the epoxy resin [11]. In this study, a supercritical water solvolysis method was considered, and the LCI data for the process were set to determine the amount of water and energy consumed for the process. The energy consumption here is the amount required to heat deionised water to a supercritical state. Inventory data for this process are provided in Table A4. From ecoinvent3 [49], the GWP of electric energy (medium voltage) in Japan is 0.176 kg CO_2eq/MJ [49], and thus, the GWP of this recycling process is 4363 kg CO_2eq/t.

Table A4. Ecoinvent3 data at solvolysis *.

Process/Material	Data	Consumption	GWP [kg CO_2eq/t]
Electricity	Market for electricity, medium voltage | JP	24,700 MJ/t	4347.2
Deionised water	Market for water, deionised, from tap water, at user | cutoff, U—RoW	10,000 L/t	15.8

* Reproduced with permission from Sommer et al., Steering Sustainable End-of-Life Treatment of Glass and Carbon Fiber Reinforced Plastics Waste from Rotor Blades of Wind Power Plants; published in 2021 [10]. Reproduced with permission from Pillain et al., Positioning supercritical solvolysis among innovative recycling and current waste management scenarios for carbon fiber reinforced plastics thanks to comparative life cycle assessment; published in 2019 [11]. Reproduced with permission from the ecoinvent Association [49].

Appendix C.5. Pyrolysis (Thermal Recycling)

Pyrolysis is a recycling method that separates the fibre reinforcement from the polymer matrix [11]. The polymer matrix is used for energy recovery in the process [11]. LCI data for electricity, nitrogen gas, and heat recovery used in pyrolysis are provided in Table A5. From ecoinvent3 [49], the GWP of electric energy (medium voltage) in Japan is 0.176 kg CO_2eq/MJ [49] and heat recovery (industrial, natural gas) is 0.0316 kg CO_2eq/MJ, and thus, the GWP of this recycling process is 3803.18 kg CO_2eq/t. The percentage of epoxy resin constituting GFRP/CFRP is 35%. The combustion of epoxy resin enables heat recovery [11].

Table A5. Ecoinvent3 data at pyrolysis *.

Process/Material	Data	Consumption	GWP [kg CO_2eq/t]
Electricity	Market for electricity, medium voltage | JP	21,125 MJ/t	3718
Nitrogen	Market for nitrogen, liquid | cutoff, U—RoW	0.699 t/t	450.156
Heat recovery	Market for heat, district or industrial, natural gas, RoW	33,000 MJ/t	−365.00

* Reproduced with permission from Sommer et al., Steering Sustainable End-of-Life Treatment of Glass and Carbon Fiber Reinforced Plastics Waste from Rotor Blades of Wind Power Plants; published in 2021 [10]. Reproduced with permission from Pillain et al., Positioning supercritical solvolysis among innovative recycling and current waste management scenarios for carbon fiber reinforced plastics thanks to comparative life cycle assessment; published in 2019 [11]. Reproduced with permission from the ecoinvent Association [49].

Appendix C.6. Fluidised Bed Process (Thermal Recycling)

This process separates the fibre reinforcement from the epoxy resin via thermal decomposition, but it is based on coal gasification [11]. The LCI data used in this study are provided in Table A6. From ecoinvent3 [49], the GWP of electric energy (medium voltage) in Japan is 0.176 kg CO_2eq/MJ [49] and heat recovery (industrial, natural gas) is 0.0316 kg CO_2eq/MJ, and thus, the GWP of this recycling process is 384.62 kg CO_2eq/t. The percentage of epoxy resin constituting GFRP/CFRP is 35%. The combustion of epoxy resin enables heat recovery [11].

Table A6. Ecoinvent3 data at fluidised bed process *.

Process/Material	Data	Consumption	GWP [kg CO_2eq/t]
Electricity	Market for electricity, medium voltage | JP	4020 MJ/t	707.52
Natural Gas	Market for heat, district or industrial, natural gas, RoW	1300 MJ/t	41.08
Heat recovery	Market for heat, district or industrial, natural gas, RoW	33,000 MJ/t	−365.00

* Reproduced with permission from Sommer et al., Steering Sustainable End-of-Life Treatment of Glass and Carbon Fiber Reinforced Plastics Waste from Rotor Blades of Wind Power Plants; published in 2021 [10]. Reproduced with permission from Pillain et al., Positioning supercritical solvolysis among innovative recycling and current waste management scenarios for carbon fiber reinforced plastics thanks to comparative life cycle assessment; published in 2019 [11]. Reproduced with permission from the ecoinvent Association [49].

Appendix C.7. Incineration

This process is a treatment method that incinerates plastic waste (mixture). We cannot find any literature applicable to this process, and thus, we applied data that were considered to be the closest from ecoinvent3 [49]. The LCI data used in this study are provided in Table A7. The GWP of this disposal process is 329 kg CO_2eq/t.

Table A7. Ecoinvent3 data at incineration *.

Process	Data	GWP [kg CO_2eq/t]
Incineration	Market for waste plastic, mixture, incineration | GLO	329

* Reproduced with permission from Sommer et al., Steering Sustainable End-of-Life Treatment of Glass and Carbon Fiber Reinforced Plastics Waste from Rotor Blades of Wind Power Plants; published in 2021 [10]. Reproduced with permission from the ecoinvent Association [49].

Appendix C.8. Landfilling

This process is a disposal method in which waste is disposed of in a sanitary landfill. This process was applied from ecoinvent3 [49] because no data that corresponded to this process were found. The LCI data used in this study are provided in Table A8. The GWP of this disposal process is 14.2 kg CO_2eq/t.

Table A8. Ecoinvent3 data at landfilling *.

Process	Data	GWP [kg CO_2eq/t]
Landfill	Market for inert waste | GLO	14.2

* Reproduced with permission from Sommer et al., Steering Sustainable End-of-Life Treatment of Glass and Carbon Fiber Reinforced Plastics Waste from Rotor Blades of Wind Power Plants; published in 2021 [10]. Reproduced with permission from the ecoinvent Association [49].

References

1. International Energy Agency Energy Statistics Data Browser. Available online: https://www.iea.org/data-and-statistics/data-tools/energy-statistics-data-browser (accessed on 20 January 2024).
2. IEA Energy Statistics Data Browser, Japan. Available online: https://www.iea.org/data-and-statistics/data-tools/energy-statistics-data-browser (accessed on 20 January 2024).
3. Global Wind Energy Council. Global Offshore Wind Report 2023. Available online: https://gwec.net (accessed on 20 January 2024).
4. United Nations. The Paris Agreement. Available online: https://www.un.org/en/climatechange/paris-agreement (accessed on 23 January 2024).
5. Masson-Delmotte, V.P.; Zhai, H.-O.; Pörtner, D.; Roberts, J.; Skea, P.R.; Shukla, A.; Pirani, W.; Moufouma-Okia, C.; Péan, R.; Pidcock, S.; et al. Global Warming of 1.5 °C. An IPCC Special Report on the Impacts of Global Warming of 1.5 °C above Pre-Industrial Levels and Related Global Greenhouse Gas Emission Pathways, in the Context of Strengthening the Global Response to the Threat of Climate Change, Sustainable Development, and Efforts to Eradicate Poverty. In IPCC. 2018, pp. 674–684. Available online: https://cir.nii.ac.jp/crid/1130574323982454028 (accessed on 23 January 2024).
6. Liu, P.; Barlow, C.Y. Wind Turbine Blade Waste in 2050. *Waste Manag.* **2017**, *62*, 229–240. [CrossRef]
7. Heng, H.; Meng, F.; McKechnie, J. Wind Turbine Blade Wastes and the Environmental Impacts in Canada. *Waste Manag.* **2021**, *133*, 59–70. [CrossRef]
8. Lichtenegger, G.; Rentizelas, A.A.; Trivyza, N.; Siegl, S. Offshore and Onshore Wind Turbine Blade Waste Material Forecast at a Regional Level in Europe until 2050. *Waste Manag.* **2020**, *106*, 120–131. [CrossRef]
9. Tazi, N.; Kim, J.; Bouzidi, Y.; Chatelet, E.; Liu, G. Waste and Material Flow Analysis in the End-of-Life Wind Energy System. *Resour. Conserv. Recycl.* **2019**, *145*, 199–207. [CrossRef]
10. Sommer, V.; Becker, T.; Walther, G. Steering Sustainable End-of-Life Treatment of Glass and Carbon Fiber Reinforced Plastics Waste from Rotor Blades of Wind Power Plants. *Resour. Conserv. Recycl.* **2022**, *181*, 106077. [CrossRef]
11. Pillain, B.; Loubet, P.; Pestalozzi, F.; Woidasky, J.; Erriguible, A.; Aymonier, C.; Sonnemann, G. Positioning Supercritical Solvolysis among Innovative Recycling and Current Waste Management Scenarios for Carbon Fiber Reinforced Plastics Thanks to Comparative Life Cycle Assessment. *J. Supercrit. Fluids* **2019**, *154*, 104607. [CrossRef]
12. Mativenga, P.T.; Shuaib, N.A.; Howarth, J.; Pestalozzi, F.; Woidasky, J. High Voltage Fragmentation and Mechanical Recycling of Glass Fibre Thermoset Composite. *CIRP Ann. Manuf. Technol.* **2016**, *65*, 45–48. [CrossRef]
13. Howarth, J.; Mareddy, S.S.R.; Mativenga, P.T. Energy Intensity and Environmental Analysis of Mechanical Recycling of Carbon Fibre Composite. *J. Clean. Prod.* **2014**, *81*, 46–50. [CrossRef]
14. Mahmud, M.A.P.; Huda, N.; Farjana, S.H.; Lang, C. Environmental Impacts of Solar-Photovoltaic and Solar-Thermal Systems with Life-Cycle Assessment. *Energies* **2018**, *11*, 2346. [CrossRef]
15. Martini, R.; Xydis, G. Repurposing and Recycling Wind Turbine Blades in the United States. *Environ. Prog. Sustain. Energy* **2023**, *42*, e13932. [CrossRef]
16. Rani, M.; Choudhary, P.; Krishnan, V.; Zafar, S. A Review on Recycling and Reuse Methods for Carbon Fiber/Glass Fiber Composites Waste from Wind Turbine Blades. *Compos. B Eng.* **2021**, *215*, 108768. [CrossRef]
17. Vo Dong, P.A.; Azzaro-Pantel, C.; Cadene, A.L. Economic and Environmental Assessment of Recovery and Disposal Pathways for CFRP Waste Management. *Resour. Conserv. Recycl.* **2018**, *133*, 63–75. [CrossRef]
18. Chen, Y.; Cai, G.; Zheng, L.; Zhang, Y.; Qi, X.; Ke, S.; Gao, L.; Bai, R.; Liu, G. Modeling Waste Generation and End-of-Life Management of Wind Power Development in Guangdong, China until 2050. *Resour. Conserv. Recycl.* **2021**, *169*, 105533. [CrossRef]
19. Liu, P.; Meng, F.; Barlow, C.Y. Wind Turbine Blade End-of-Life Options: An Eco-Audit Comparison. *J. Clean. Prod.* **2019**, *212*, 1268–1281. [CrossRef]
20. Krauklis, A.E.; Karl, C.W.; Gagani, A.I.; Jørgensen, J.K. Composite Material Recycling Technology—State-of-the-Art and Sustainable Development for the 2020s. *J. Compos. Sci.* **2021**, *5*, 28. [CrossRef]
21. Wei, Y.; Hadigheh, S.A. Cost Benefit and Life Cycle Analysis of CFRP and GFRP Waste Treatment Methods. *Constr. Build. Mater.* **2022**, *348*, 128654. [CrossRef]
22. Zhu, D.; Mortazavi, S.M.; Maleki, A.; Aslani, A.; Yousefi, H. Analysis of the Robustness of Energy Supply in Japan: Role of Renewable Energy. *Energy Rep.* **2020**, *6*, 378–391. [CrossRef]
23. Ministry of Economy, Trade and Industry. Electric Power Survey Statistics 2018, 2019, 2020. Available online: https://www.enecho.meti.go.jp/statistics/electric_power/ep002/results.html (accessed on 24 January 2024).
24. Prime Minister's Office in Japan Prime Minister Kan's Policy Speech at the 203rd Session of the Diet. Available online: https://www.kantei.go.jp/jp/99_suga/statement/2020/1026shoshinhyomei.html (accessed on 27 July 2023).
25. Ministry of Economy, Trade and Industry. Basic Energy Plan. 2021. Available online: https://www.enecho.meti.go.jp/category/others/basic_plan/pdf/20211022_01.pdf (accessed on 24 January 2024).
26. Oshiro, K.; Fujimori, S.; Ochi, Y.; Ehara, T. Enabling Energy System Transition toward Decarbonization in Japan through Energy Service Demand Reduction. *Energy* **2021**, *227*, 120464. [CrossRef]
27. Kuriyama, A.; Liu, X.; Naito, K.; Tsukui, A.; Tanaka, Y. Importance of Long-Term Flexibility in a 100% Renewable Energy Scenario for Japan. *Sustain. Sci.* **2023**, *19*, 165–187. [CrossRef]

28. Fragkos, P.; Laura van Soest, H.; Schaeffer, R.; Reedman, L.; Köberle, A.C.; Macaluso, N.; Evangelopoulou, S.; De Vita, A.; Sha, F.; Qimin, C.; et al. Energy System Transitions and Low-Carbon Pathways in Australia, Brazil, Canada, China, EU-28, India, Indonesia, Japan, Republic of Korea, Russia and the United States. *Energy* **2021**, *216*, 119385. [CrossRef]
29. Sugiyama, M.; Fujimori, S.; Wada, K.; Oshiro, K.; Kato, E.; Komiyama, R.; Silva Herran, D.; Matsuo, Y.; Shiraki, H.; Ju, Y. EMF 35 JMIP Study for Japan's Long-Term Climate and Energy Policy: Scenario Designs and Key Findings. *Sustain. Sci.* **2021**, *16*, 355–374. [CrossRef]
30. Xu, Y.; Li, J.; Tan, Q.; Peters, A.L.; Yang, C. Global Status of Recycling Waste Solar Panels: A Review. *Waste Manag.* **2018**, *75*, 450–458. [CrossRef] [PubMed]
31. Asia-Pacific Integrated Model Project Team a Trial Calculation of the Realization of a Decarbonized Society in 2050. Available online: https://www.enecho.meti.go.jp/committee/council/basic_policy_subcommittee/034/034_004.pdf (accessed on 20 January 2024).
32. Japan Wind Power Association Disposal and Recycling of Wind Power Generation Equipment. Available online: https://www.meti.go.jp/shingikai/energy_environment/disposal_recycle/pdf/004_04_00.pdf (accessed on 24 January 2024).
33. New Energy and Industrial Technology Development Organization Wind Power Generation Facilities and Installations in Japan. Available online: https://www.nedo.go.jp/library/fuuryoku/reference.html (accessed on 20 January 2024).
34. Goedkoop, M.; Oele, M.; Leijting, J.; Ponsioen, T.; Meijer, E. Introduction to LCA with SimaPro. Available online: https://pre-sustainability.com/legacy/download/SimaPro8IntroductionToLCA.pdf (accessed on 24 January 2024).
35. Hibino, G.; Pandey, R.; Matsuoka, Y.; Kainuma, M. Climate Policy Assessment: Asia-Pacific Integrated Modeling. In *A Guide to AIM/Enduse Model BT*; Kainuma, M., Matsuoka, Y., Morita, T., Eds.; Springer: Tokyo, Japan, 2003; pp. 247–398. ISBN 978-4-431-53985-8.
36. The International Institute for Applied Systems Analysis (IIASA) LED Database (Version 1.0). Available online: https://db1.ene.iiasa.ac.at/LEDDB (accessed on 22 February 2024).
37. Díaz, H.; Guedes Soares, C. Review of the Current Status, Technology and Future Trends of Offshore Wind Farms. *Ocean Eng.* **2020**, *209*, 107381. [CrossRef]
38. Grubler, A.; Wilson, C.; Bento, N.; Boza-Kiss, B.; Krey, V.; McCollum, D.L.; Rao, N.D.; Riahi, K.; Rogelj, J.; De Stercke, S.; et al. A Low Energy Demand Scenario for Meeting the 1.5 °C Target and Sustainable Development Goals without Negative Emission Technologies. *Nat. Energy* **2018**, *3*, 515–527. [CrossRef]
39. Cao, Z.; O'Sullivan, C.; Tan, J.; Kalvig, P.; Ciacci, L.; Chen, W.; Kim, J.; Liu, G. Resourcing the Fairytale Country with Wind Power: A Dynamic Material Flow Analysis. *Environ. Sci. Technol.* **2019**, *53*, 11313–11322. [CrossRef] [PubMed]
40. Mishnaevsky, L. Sustainable End-of-Life Management of Wind Turbine Blades: Overview of Current and Coming Solutions. *Materials* **2021**, *14*, 1124. [CrossRef] [PubMed]
41. Zimmermann, T.; Rehberger, M.; Gößling-Reisemann, S. Material Flows Resulting from Large Scale Deployment of Wind Energy in Germany. *Resources* **2013**, *2*, 303–334. [CrossRef]
42. Wang, Y.; Sun, T. Life Cycle Assessment of CO_2 Emissions from Wind Power Plants: Methodology and Case Studies. *Renew. Energy* **2012**, *43*, 30–36. [CrossRef]
43. Crawford, R.H. Life Cycle Energy and Greenhouse Emissions Analysis of Wind Turbines and the Effect of Size on Energy Yield. *Renew. Sustain. Energy Rev.* **2009**, *13*, 2653–2660. [CrossRef]
44. Lenzen, M.; Munksgaard, J. Energy and CO_2 Life-Cycle Analyses of Wind Turbines—Review and Applications. *Renew. Energy* **2002**, *26*, 339–362. [CrossRef]
45. Ribrant, J.; Bertling, L. Survey of Failures in Wind Power Systems with Focus on Swedish Wind Power Plants during 1997–2005. In Proceedings of the 2007 IEEE Power Engineering Society General Meeting, Tampa, FL, USA, 24–28 June 2007; pp. 1–8.
46. Andersen, N.; Eriksson, O.; Hillman, K.; Wallhagen, M. Wind Turbines' End-of-Life: Quantification and Characterisation of Future Waste Materials on a National Level. *Energies* **2016**, *9*, 999. [CrossRef]
47. Akita Offshore Wind Power Co. Business Overview. Available online: https://aow.co.jp/jp/project/ (accessed on 24 January 2024).
48. Japan Plastic Recycling and Reuse Association Production, Disposal, Recycling, Treatment and Disposal of Plastic Products in Japan. Available online: https://www.pwmi.or.jp/pdf/panf2.pdf (accessed on 24 January 2024).
49. Ecoinvent Association Ecoinvent Database 3. Available online: https://ecoinvent.org/ (accessed on 20 January 2024).
50. Ecoinvent Association Implementation of Life Cycle Impact Assessment Methods in the Ecoinvent Database v3.9 (2022.10.13). Available online: https://support.ecoinvent.org/ecoinvent-version-3.9 (accessed on 24 January 2024).
51. e-Stat Total Amount of Industrial Waste in the Electricity Industry in 2020. Available online: https://www.e-stat.go.jp/stat-search/files?page=1&layout=datalist&toukei=00650102&tstat=000001204240&cycle=8&tclass1val=0 (accessed on 25 January 2024).
52. Imamura, E.; Iuchi, M.; Bando, S. *Comprehensive Assessment of Life Cycle CO_2 Emissions from Power Generation Technologies in Japan*; Central Research Institute of Electric Power Industry: Tokyo, Japan, 2014; pp. 1–85.
53. Pickering, S.J. Recycling Technologies for Thermoset Composite Materials-Current Status. *Compos. Part A Appl. Sci. Manuf.* **2006**, *37*, 1206–1215. [CrossRef]